



Original Article

# Impacts of surface characteristics on biological responses and biofilm formation of 3D-printed denture base resins: An in vitro study



Chien-Fu Tseng <sup>a,b,c†</sup>, Chia-Chih Sung <sup>b,c†</sup>, Ya-Ting Yang <sup>d†</sup>,  
Fen-Ni Chen <sup>e</sup>, Yuichi Mine <sup>g</sup>, Yao-Chang Chiang <sup>h,i</sup>,  
Zih-Chan Lin <sup>h</sup>, Mei-Ling Fang <sup>j,k</sup>, Hsin-Ming Chen <sup>a,l,m</sup>,  
Sang-Heng Kok <sup>a,m</sup>, Tzu-Yu Peng <sup>f\*</sup>

<sup>a</sup> Graduate Institute of Clinical Dentistry, School of Dentistry, College of Medicine, National Taiwan University, Taipei, Taiwan

<sup>b</sup> Department of Dentistry, Taoyuan General Hospital, Ministry of Health and Welfare, Taoyuan, Taiwan

<sup>c</sup> Research Center for Tooth Bank and Dental Stem Cell Technology, College of Oral Medicine, Taipei Medical University, Taipei, Taiwan

<sup>d</sup> Department of Dentistry, Taipei Medical University Shuang Ho Hospital, New Taipei City, Taiwan

<sup>e</sup> School of Dental Technology, College of Oral Medicine, Taipei Medical University, Taipei, Taiwan

<sup>f</sup> School of Dentistry, College of Oral Medicine, Taipei Medical University, Taipei, Taiwan

<sup>g</sup> Department of Medical Systems Engineering, Hiroshima University Graduate School of Biomedical and Health Sciences, Hiroshima City, Japan

<sup>h</sup> Chronic Diseases and Health Promotion Research Center, Center for Drug Research and Development, Chang Gung University of Science and Technology, Chiayi, Taiwan

<sup>i</sup> Department of Nursing, Division of Basic Medical Sciences, Chang Gung University of Science and Technology, Chiayi, Taiwan

<sup>j</sup> Center for Environmental Toxin and Emerging-Contaminant Research, Cheng Shiu University, Kaohsiung, Taiwan

<sup>k</sup> Department of Civil Engineering and Geomatics, Cheng Shiu University, Kaohsiung, Taiwan

<sup>l</sup> Graduate Institute of Oral Biology, School of Dentistry, College of Medicine, National Taiwan University, Taipei, Taiwan

<sup>m</sup> Department of Dentistry, National Taiwan University Hospital, College of Medicine, National Taiwan University, Taipei, Taiwan

Received 21 March 2025

Available online 4 April 2025

\* Corresponding author. School of Dentistry, College of Oral Medicine, Taipei Medical University, 250 Wu-Hsing Street, Taipei 11031, Taiwan.

E-mail address: [typeng@tmu.edu.tw](mailto:typeng@tmu.edu.tw) (T.-Y. Peng).

† These three authors contributed equally to this study.

**KEYWORDS**

3D printing;  
Denture base resin;  
Cell viability;  
Biofilm formation;  
Surface characteristics

**Abstract** *Background/purpose:* With advancements in digital technology, fully digital workflow for complete denture fabrication using 3D-printed denture base resin (DBR) has gained increasing clinical acceptance in recent years. However, the surface characteristics, biocompatibility, and biofilm formation of 3D-printed DBR materials remain insufficiently understood. Therefore, in this study, we investigated and analyzed these aspects.

**Materials and methods:** Disk-shaped DBR specimens ( $\varnothing$  2.5 mm, 3 mm thick) were fabricated using packed (PA), milled (ML), and 3D-printed (3D) processes. All specimens were ground with silicon carbide sandpaper (#600) and ultrasonically cleaned. Surface microtopography and sub-micron roughness were analyzed using scanning electron microscopy and atomic force microscopy, while a goniometer was used to measure contact angles to calculate the surface energy. Human gingival fibroblasts and *Aggregatibacter actinomycetemcomitans* were cultured on the specimens to assess the cytotoxicity and biofilm formation. Statistical analyses were performed with a significance level set to 0.05.

**Results:** Microscopic imaging revealed that the 3D group exhibited a more uniformly distributed texture, while it also had the lowest surface roughness (0.85  $\mu\text{m}$ ). Additionally, the PA group had the most hydrophobic surface ( $82.47^\circ$ ) and the highest surface free energy (46.08 mN/m). Notably, no group showed cytotoxic effects after 72 h of testing. In addition, the 3D group demonstrated the lowest biofilm formation after both 24 h and 72 h of microbial culture.

**Conclusion:** 3D-printed DBRs exhibited the lowest surface roughness, maintaining non-cytotoxic and superior resistance to microbial adhesion, suggesting their potential for complete denture fabrication, easy maintenance of oral hygiene, and long-term clinical performance.

© 2025 Association for Dental Sciences of the Republic of China. Publishing services by Elsevier B.V. This is an open access article under the CC BY-NC-ND license (<http://creativecommons.org/licenses/by-nc-nd/4.0/>).

## Introduction

For edentulous patients whose treatment options are limited due to systemic conditions, oral health status, or financial constraints, complete dentures remain the treatment of choice.<sup>1</sup> Denture base resin (DBR), as the primary material for complete dentures, must exhibit excellent mechanical strength, biocompatibility, and stability to ensure long-term durability and patient comfort.<sup>2,3</sup> Currently, polymethyl methacrylate (PMMA) remains the most commonly used DBR in clinical practice due to its ease of processing, esthetic properties, cost-effectiveness, and adequate mechanical performance.<sup>4</sup> Conventional fabrication methods for DBRs primarily include cold-curing and heat-curing polymerization. Cold-cured DBRs are polymerized through chemical self-curing, offering convenient handling;<sup>5</sup> however, they tend to have higher residual monomer contents.<sup>6</sup> In contrast, heat-cured DBRs undergo polymerization under elevated temperature and pressure, effectively reducing porosity and enhancing flexural strength and wear resistance.<sup>7</sup> Nonetheless, the heat-curing process still suffers from polymerization shrinkage, which compromises the fit of the denture.<sup>8</sup> Additionally, the conventional fabrication workflow is complex and requires highly skilled technicians. Therefore, improving the properties of DBRs while simplifying the manufacturing process has become a crucial area of development in digital dental technology.<sup>9–11</sup>

The full digitalization of denture fabrication workflows has emerged as a significant trend in recent years, leading

to notable improvements in both efficiency and precision.<sup>10–12</sup> Among these advancements, milling and three-dimensional (3D) printing are the most representative digital manufacturing techniques. The milling process utilizes pre-polymerized PMMA blocks for high-precision cutting, which not only enhances the fitting accuracy of dentures and minimizes the deformation issues associated with conventional heat-curing processes but reduces the release of residual monomers.<sup>13,14</sup> However, milling results in considerable material waste and involves high equipment costs.<sup>15,16</sup> In comparison, 3D printing reduces material waste through layer-by-layer photopolymerization and enables the fabrication of DBRs with complex geometries and customized designs.<sup>16–18</sup> While digital manufacturing techniques have significantly advanced DBR applications, most research has focused on comparing the mechanical properties, dimensional accuracy, and color stability of conventionally packed, milled, or 3D-printed DBRs; yet comprehensive evaluations of their biocompatibility and biofilm formation remain limited.

To our knowledge, only a few 3D-printed DBR materials or brands have received medical device licenses from the Taiwanese government or international regulatory agencies, highlighting the need for further investigation. Therefore, in this study, we analyzed the surface characteristics, biocompatibility, and biofilm formation of DBRs fabricated using three different processes: conventional cold-polymerized packing (SR Triplex Cold), milling (IvoBase CAD Pink V), and 3D printing (FREEPRINT denture). The findings will provide scientific evidence for evaluating the

clinical safety and feasibility of 3D-printed DBRs and contribute to the advancement of fully digital denture fabrication technologies.

## Materials and methods

### Fabrication of test specimens

Disk-shaped samples ( $\phi$ 10.0 mm, 3.0 mm thick) were fabricated using conventional packing (PA), five-axis milling (ML), and 3D printing (3D) processes. The materials used and fabrication methods in this study are listed in Table 1. All samples were ground with silicon carbide paper, cleaned with distilled water in an ultrasonic cleaner, and air-dried.

### Surface characterization

Surface microtopography was observed using a thermal field emission scanning electron microscope (FE-SEM; JSM-7800F Prime, JEOL, Tokyo, Japan), with images recorded at  $2500 \times$  and  $5000 \times$  magnification. An atomic force microscope (AFM; Bruker Dimension Icon VT-1000, Santa Barbara, CA, USA) was used to measure submicron surface roughness over a  $5 \times 5\text{-}\mu\text{m}$  area ( $n = 10$ ). Contact angles of distilled water ( $CA_w$ ) and diiodomethane ( $CA_d$ ) were measured on 10 specimens per group using a goniometer (Phoenix Mini, Surface Electro Optics, Seoul, South Korea), with three  $10 \mu\text{L}$  drops of each liquid measured per specimen. The surface energy (SE) was further calculated using the method of Owens, Wendt, Rabel and Kaelble via Surfaceware software (vers. 9, Surface Electro Optics) based on contact angle data.

### Cell cultures and cell cytotoxicity

The human gingival fibroblast (HGF-1) cell line (ATCC #CRL-2014) was cultured in Dulbecco's modified Eagle medium (DMEM), following a method described by Peng et al.<sup>19</sup> Autoclaved specimens ( $121^\circ\text{C}$ ,  $1.2 \text{ kg/cm}^2$ , 30 min) from each processing were immersed in DMEM at  $37^\circ\text{C}$  for 72 h to prepare extracts for the cytotoxicity assay. HGF-1 cells

were seeded in a 96-well plate (at  $10^6$  cells/well). After cell attachment, the culture medium was replaced with DMEM containing specimen extracts. After 24 h of incubation, cell viability was assessed using the PrestoBlue reagent according to the manufacturer's instructions.

### Microbial cultures and biofilm formation assay

An *Aggregatibacter actinomycetemcomitans* microbial strain (BCRC #80375) was cultured in brain heart infusion broth, following a method described by Peng et al.<sup>20</sup> The optical density at 600 nm (OD600) was adjusted to 1.0 using fresh broth to obtain a standard inoculum of  $3 \times 10^8$  colony-forming units (CFU)/mL. *Aggregatibacter actinomycetemcomitans* ( $10^6$  CFU/mL) was inoculated into all wells of a 24-well plate containing DBR samples (PA, ML, or 3D) and incubated at  $37^\circ\text{C}$  for 24 h and 72 h. After incubation, the medium was removed, and wells were washed twice with phosphate-buffered saline (PBS) and air-dried for 1 h. Crystal violet (150  $\mu\text{L}$  of 0.1 % w/v) was added to each well and incubated at room temperature for 10–15 min. The absorbance at 490 nm (OD490) was measured on an enzyme-linked immunosorbent assay (ELISA) microplate reader (Molecular Devices, San Jose, CA, USA).

### Statistical analysis

Data are expressed as the mean  $\pm$  standard deviation (SD). Normality was confirmed using the Shapiro–Wilk test, allowing for parametric analysis. Ra values and hydrophilicity comparisons were conducted using a one-way analysis of variance (ANOVA), followed by Tukey's post-hoc honest significant difference (HSD) test for multiple group comparisons (PA, ML, and 3D). Biological evaluation assays (cytotoxicity and biofilm formation) were performed with three replicates per group and analyzed using a one-way ANOVA with Tukey's HSD post-hoc test. Statistical analyses were conducted using SPSS (vers. 19, IBM, Amork, NY, USA) and Prism (vers. 10, GraphPad Software, San Diego, CA, USA), with significance set to  $P < 0.05$ .

**Table 1** Materials used in this study.

Identification (Manufacturer)	Composition <sup>a</sup>	Fabrication process	Machine (Manufacturer)	Abbreviation
SR triplex cold (ivoclar Vivadent AG, Schaan, Liechtenstein)	Powder: PMMA, catalyst, pigments Liquid: MMA, dimethacrylate, catalyst, stabilizer	Conventional packing (self-curing)	—	PA
IvoBase CAD Pink V (ivoclar Vivadent AG, Schaan, Liechtenstein)	PMMA, co-polymer for impact toughness modification, pigments	Universal five-axis production unit	inLab MC X5 (Dentsply Sirona, long island City, NY, USA)	ML
FREEPRINT denture (Detax, Ettlingen, Germany)	—	DLP light-curing 3D printer	3Demax (DMG medical devices, Hamburg, Germany)	3D

PMMA, polymethylmethacrylate; MMA, methylmethacrylate; DLP, digital light processing.

<sup>a</sup> Composition information was provided by the manufacturer, while the 3D printing manufacturer did not provide the detailed composition.

## Results

### Surface microtopography and topography

Based on microscopic images shown in **Fig. 1**, all specimens exhibited distinct linear grinding marks. The PA group showed the most pronounced texture, the ML group featured parallel deep grooves, and the 3D group presented a uniformly distributed microstructure. The surface roughness and topography of the DBRs are summarized in **Table 2** and **Fig. 1**. The Ra value of the PA group was significantly higher than those of the ML and 3D groups ( $P < 0.05$ ), and Rq values followed a similar trend, indicating that the PA group exhibited greater surface microtopographical variations and more-pronounced height fluctuations. Rz, which represents the maximum height roughness, was greatest in the PA group, followed by the ML and 3D groups, with a significant difference between the PA and 3D groups ( $P < 0.05$ ).

### Surface wettability

The surface wettability results are presented in **Table 2**. CA<sub>W</sub>, which reflects the surface wettability to polar liquids, was significantly lower in the PA group than in the ML and 3D groups ( $P < 0.05$ ), indicating higher hydrophilicity. CA<sub>D</sub>, representing wettability to non-polar liquids, ranged 25.92°–28.88°, with no significant differences among the three groups ( $P > 0.13$ ). Although the PA group exhibited a lower CA<sub>W</sub> value, no significant differences in SE were observed among the three groups ( $P > 0.24$ ).

### Cytotoxicity

The cytotoxicity assessment results (**Fig. 2**) showed no significant differences in cell viabilities among the processing groups compared to the blank group (NT) at any

time points ( $P > 0.95$ ). This indicated that different DBR fabrication processes did not induce immediate or intermediate cytotoxicity in HGF-1 cells. Cell viability remained stable, confirming the excellent cytocompatibility of DBR materials and the absence of significant cytotoxic substance release.

### Biofilm formation

**Fig. 3** illustrates *A. actinomycetemcomitans* biofilm formation on DBRs fabricated using the three processes. The PA group exhibited significantly greater biofilm formation at 72 h than at 24 h ( $P < 0.05$ ), indicating a clear accumulation trend over time. In contrast, the ML and 3D groups showed minimal variations between 24 h and 72 h ( $P > 0.06$ ), suggesting more-stable bacterial adhesion. Notably, the 3D group demonstrated the lowest biofilm formation at both time points compared to the PA and ML groups, suggesting that the surface characteristics of the 3D-printed DBRs may inhibit *A. actinomycetemcomitans* adhesion.

## Discussion

Compared to conventional packing (self-curing) and five-axis milling, digital light processing (DLP) 3D printing significantly reduces the surface roughness of DBRs. This improvement stems from its high-precision layer-by-layer stacking, the self-leveling effect of liquid resin, reduced mechanical stresses, and controlled post-processing.<sup>21,22</sup> DLP technology employs a digital light source to simultaneously cure the entire resin layers, achieving a minimum layer thickness of 50  $\mu\text{m}$ , which enhances surface smoothness.<sup>23</sup> The liquid resin fills minor irregularities before photopolymerization, minimizing defects.<sup>21–23</sup> In contrast, conventional packing is prone to polymerization shrinkage, air bubbles, and mold limitations, while milling introduces tool marks, increasing roughness.<sup>5,6,15,16</sup> Additionally, DLP

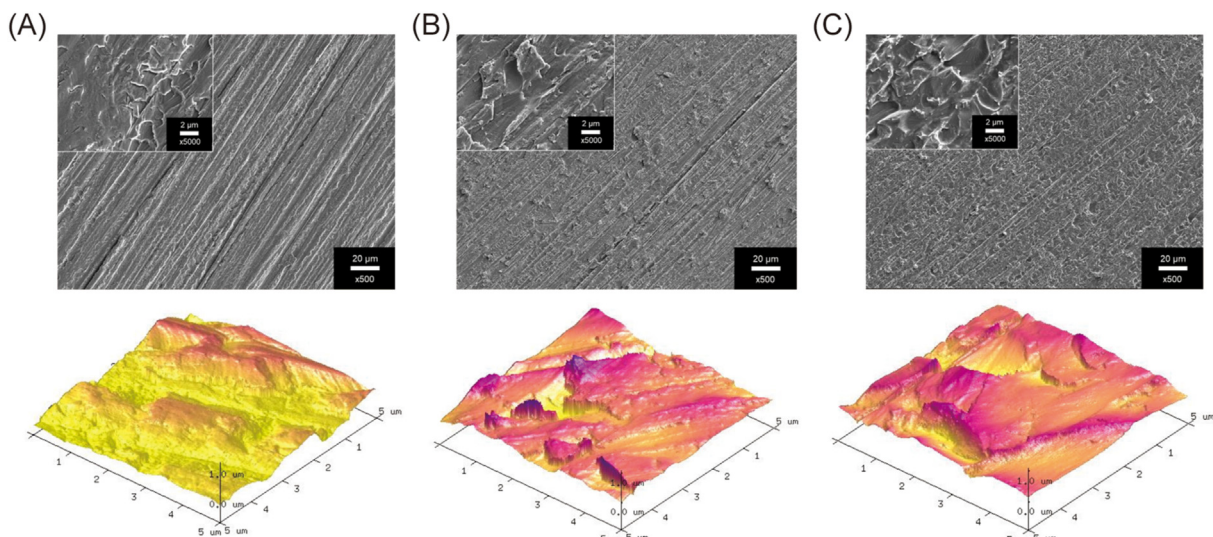


**Figure 1** Surface microtopography and topography of denture base resins (DBRs) fabricated using (A) conventional packing, (B) a universal five-axis production unit, and (C) a digital light processing (DLP) light-curing 3D printer.

eliminates tool-induced microcracks and scratches. Post-processing, including isopropanol cleaning and secondary curing, further reduces roughness. The uniform cross-linked molecular structure formed during DLP printing minimizes microscopic defects, ensuring superior surface quality compared to thermosetting or self-polymerizing resins.<sup>23–25</sup>

To the best of our knowledge, most 3D-printable DBRs are primarily designed for provisional (temporary) or immediate dentures. However, the FREEPRINT denture (Detax) used in this study is the material that has received approval from the US Food and Drug Administration and European Union Medical Devices Regulation, allowing its use in definitive dentures. Given its long-term clinical application, it is crucial to further evaluate its biocompatibility, as potential cytotoxicity may arise from the release of unpolymerized monomers, residual polymerization initiators, or other degradation byproducts.<sup>6,13,14</sup> In this study, none of the tested DBR materials induced significant cytotoxic reactions (Fig. 2), indicating that their chemical composition and fabrication processes support stable cell growth without adverse effects on HGF-1 cells. The observed stable cell viability and favorable biocompatibility further reinforced the clinical safety of these materials, supporting their feasibility for use in definitive denture fabrication.<sup>26</sup>

Surface roughness plays a crucial role in determining the wettability and bacterial adhesion characteristics of materials.<sup>1,27</sup> The PA group exhibited higher Ra and Rz values (Table 2), indicating a greater degree of surface

microtopography, which may promote moisture retention and the exposure of polar functional groups such as hydroxyl (–OH) and carboxyl (–COOH), thereby increasing hydrophilicity (lower CA<sub>W</sub>).<sup>28,29</sup> Hydrophilic surfaces tend to more readily adsorb water and biomolecules, such as proteins, providing initial conditions favorable for bacterial adhesion.<sup>30,31</sup> The pronounced surface polarity of the PA group may facilitate early bacterial colonization and accelerate biofilm development. Studies showed that moderately hydrophilic surfaces create a conducive wetting environment for bacterial adhesion and proliferation,<sup>32</sup> which explains the significant increase in biofilm formation in the PA group within 72 h. In contrast, the ML and 3D groups exhibited significantly higher CA<sub>W</sub> values than the PA group, indicating greater hydrophobicity. Notably, the 3D group displayed the lowest Ra, Rq, and Rz values (Table 2), resulting in the smoothest surface, which may have further influenced the bacterial adhesion behavior. Generally, smoother surfaces reduce microscopic pores and depressions, making it more difficult for bacteria to establish stable attachment and aggregation, thereby limiting biofilm accumulation.<sup>32</sup> The specific micro-layered structure generated by 3D printing may also affect the water contact angle and bacterial adhesion mechanisms, which may have led to lower biofilm formation at both 24 h and 72 h compared to the PA and ML groups.<sup>33</sup> This suggests that 3D-printed DBRs may inhibit the adhesion of periodontal pathogens.

**Table 2** Surface roughness and wettability of the denture base resins (DBRs).

Group	Surface roughness			Surface wettability		
	Ra (μm)	Rq (μm)	Rz (μm)	CA <sub>W</sub> (°)	CA <sub>D</sub> (°)	SE (mN/m)
PA	0.90 ± 0.16 <sup>a</sup>	1.14 ± 0.28 <sup>a</sup>	6.40 ± 1.75 <sup>a</sup>	82.47 ± 1.44 <sup>a</sup>	25.92 ± 0.68 <sup>a</sup>	46.09 ± 0.43 <sup>a</sup>
ML	0.84 ± 0.11 <sup>b</sup>	1.02 ± 0.13 <sup>b</sup>	6.01 ± 1.40 <sup>a,b</sup>	86.43 ± 1.16 <sup>b</sup>	26.69 ± 2.42 <sup>a</sup>	45.34 ± 0.95 <sup>a</sup>
3D	0.83 ± 0.14 <sup>b</sup>	1.03 ± 0.14 <sup>b</sup>	5.73 ± 0.88 <sup>b</sup>	85.05 ± 1.98 <sup>b</sup>	28.88 ± 3.99 <sup>a</sup>	44.64 ± 1.75 <sup>a</sup>

DBRs were fabricated using conventional packing (PA), a universal five-axis production unit (ML), and a DLP light-curing 3D printer (3D). Ra, arithmetic mean deviation; Rq, root mean square deviation; Rz, maximum height of profile; CA<sub>W</sub>, contact angle of distilled water; CA<sub>D</sub>, contact angle of diiodomethane; SE, surface energy.

<sup>a</sup> and <sup>b</sup>: Different superscript letters in the same column indicate a significant difference in the mean of the parameter between the two groups.

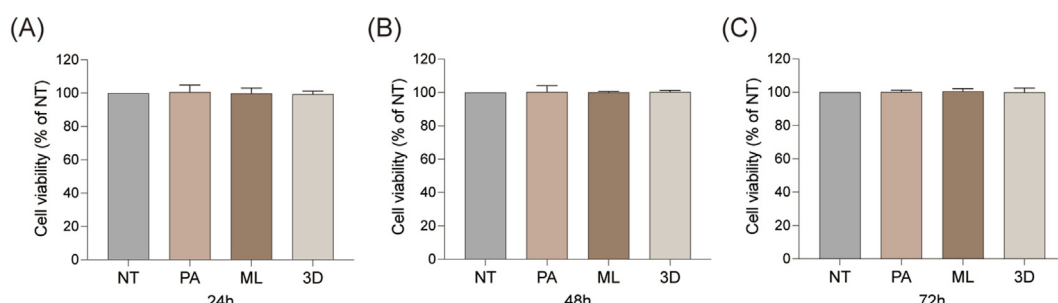


**Figure 2** Assessment of human gingival fibroblast (HGF-1) cytotoxicity on denture base resin (DBR) surfaces after (A) 24 h, (B) 48 h, and (C) 72 h, as determined using the PrestoBlue cell viability reagent. NT, blank group without a DBR specimen; DBRs were fabricated using conventional packing (PA), a universal five-axis production unit (ML), and a digital light processing (DLP) light-curing 3D printer (3D).

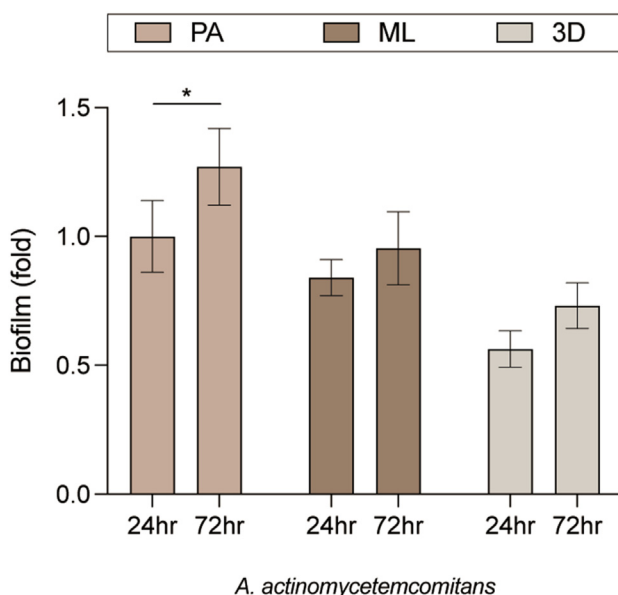


**Figure 3** Biofilm formation ability of *A. actinomycetemcomitans* on denture base resin (DBR) surfaces fabricated using conventional packing (PA), a universal five-axis production unit (ML), and a digital light processing (DLP) light-curing 3D printer (3D). \* Significantly differs from PA at 24 h and 72 h ( $P < 0.05$ ).

It is noteworthy that biofilm formation on DBR surfaces is closely associated with surface roughness values.<sup>34</sup> Previous studies demonstrated that when the Ra of resin exceeds the clinically acceptable threshold of 0.2  $\mu\text{m}$ , bacterial adhesion and biofilm formation significantly increase.<sup>35</sup> Therefore, controlling the surface roughness of DBR materials below this threshold is essential for minimizing bacterial attachment and preventing biofilm-associated infections. However, in this study, all DBR samples were subjected only to sandpaper polishing without additional polishing treatments, resulting in surface roughness values exceeding the threshold. Consequently, biofilm formation was observed on all material surfaces, consistent with previous research findings. This highlights an important clinical recommendation that DBR should undergo appropriate polishing procedures to reduce surface roughness and prevent microbial adhesion in clinical applications.

There are several limitations in this study, including optical properties, water absorption, and dimensional stability of 3D-printed DBRs which were not investigated. Additionally, the biocompatibility and biofilm formation assays utilized only a single cell line and microbial strain, which might not comprehensively reflect the complex oral microbiome and clinical environment. Future research should further explore these factors to obtain more-complete evaluations. Despite these limitations, the findings of this study indicate that DBRs fabricated using different manufacturing processes (PA, ML, and 3D) exhibited good biocompatibility, and that surface wettability and roughness significantly influence biofilm formation. Due to its higher hydrophobicity and lower surface roughness, 3D-printed DBRs may reduce moisture retention and bacterial adhesion, leading to more-stable biofilm

formation and lower bacterial counts over time compared to other manufacturing methods. This suggests that its surface characteristics may help mitigate biofilm development, thereby reducing the risk of infection and biofilm-associated complications. Overall, 3D printing technology provides a simple and efficient method for DBR fabrication, and the findings of this study can serve as a valuable reference for clinical applications and material selection.

### Declaration of competing interest

The authors have no conflicts of interest relevant to this article.

### Acknowledgments

This work was supported by research grants from the National Science and Technology Council of Taiwan (112-2314-B-038-118-MY2), Division of Research Planning and Development, Department of Research and Development, Taoyuan General Hospital, Ministry of Health and Welfare (PTH114058), and the College of Oral Medicine, Taipei Medical University (TMUCOM202402).

### References

1. Gad MA, Abdelhamid AM, ElSamahy M, et al. Effect of aging on dimensional accuracy and color stability of CAD-CAM milled and 3D-printed denture base resins: a comparative *in vitro* study. *BMC Oral Health* 2024;24:1124.
2. Paulino MR, Alves LR, Gurgel BCV, et al. Simplified versus traditional techniques for complete denture fabrication: a systematic review. *J Prosthet Dent* 2015;113:12–6.
3. Alqtaibi AY, Baik A, Almuzaini SA, et al. Polymeric denture base materials: a review. *Polymers* 2023;15:3258.
4. Alp G, Johnston WM, Yilmaz B. Optical properties and surface roughness of prepolymerized poly(methyl methacrylate) denture base materials. *J Prosthet Dent* 2019;121:347–52.
5. Zafar MS. Prosthodontic applications of polymethyl methacrylate (PMMA): an update. *Polymers* 2020;12:2299.
6. Taylor PB, Frank SL. Low temperature polymerization of acrylic resins. *J Dent Res* 1950;29:486–92.
7. Ferracane JL. Hygroscopic and hydrolytic effects in dental polymer networks. *Dent Mater* 2006;22:211–22.
8. Lee S, Hong SJ, Paek J, et al. Comparing accuracy of denture bases fabricated by injection molding, CAD/CAM milling, and rapid prototyping method. *J Adv Prosthodont* 2019;11:55–64.
9. Temizci T, Bozoğulları HN. Effect of thermal cycling on the flexural strength of 3-D printed, CAD/CAM milled and heat-polymerized denture base materials. *BMC Oral Health* 2024;24:357.
10. Yu HJ, Kang YJ, Park Y, et al. A comparison of the mechanical properties of 3D-printed, milled, and conventional denture base resin materials. *Dent Mater J* 2024;43:813–21.
11. Arora O, Ahmed N, Nallaswamy D, et al. Denture base materials: an *in vitro* evaluation of the mechanical and color properties. *J Dent* 2024;145:104993.
12. Abualsaud R, Gad MM. Flexural strength of CAD/CAM denture base materials: systematic review and meta-analysis of in-vitro studies. *J Int Soc Prev Community Dent* 2022;12:160–70.
13. Batisse C, Nicolas E. Comparison of CAD/CAM and conventional denture base resins: a systematic review. *Appl Sci* 2021;11: 5990.

14. Takhtdar M, Azizimoghadam N, Kalantari MH, et al. Effect of denture cleansers on color stability and surface roughness of denture bases fabricated from three different techniques: conventional heat-polymerizing, CAD/CAM additive, and CAD/CAM subtractive manufacturing. *Clin Exp Dent Res* 2023;9:840–50.
15. Dimitrova M, Corsalini M, Kazakova R, et al. Comparison between conventional PMMA and 3D printed resins for denture bases: a narrative review. *J Compos Sci* 2022;6:87.
16. Sidhom M, Zaghloul H, Mosleh IE, et al. Effect of different CAD/CAM milling and 3D printing digital fabrication techniques on the accuracy of PMMA working models and vertical marginal fit of PMMA provisional dental prosthesis: an in vitro study. *Polymers* 2022;14:1285.
17. Jeong YG, Lee WS, Lee KB. Accuracy evaluation of dental models manufactured by CAD/CAM milling method and 3D printing method. *J Adv Prosthodont* 2018;10:245–51.
18. Etemad-Shahidi Y, Qallandar OB, Evenden J, et al. Accuracy of 3-dimensionally printed full-arch dental models: a systematic review. *J Clin Med* 2020;9:3357.
19. Peng TY, Ma TL, Lee IT, et al. Enhancing dental cement bond strength with autofocus-laser-cutter-generated grooves on polyetheretherketone surfaces. *Polymers* 2023;15:3670.
20. Peng TY, Lin DJ, Mine Y, et al. Biofilm formation on the surface of (poly)ether-ether-ketone and in vitro antimicrobial efficacy of photodynamic therapy on peri-implant mucositis. *Polymers* 2021;13:940.
21. Kaushik A, Garg RK. Effect of printing parameters on the surface roughness and dimensional accuracy of digital light processing fabricated parts. *J Mater Eng Perform* 2024;33: 11863–75.
22. Kang JW, Jeon J, Lee JY, et al. Surface-wetting characteristics of DLP-based 3D printing outcomes under various printing conditions for microfluidic device fabrication. *Micromachines* 2024;15:61.
23. Zhang ZC, Li PL, Chu FT, et al. Influence of the three-dimensional printing technique and printing layer thickness on model accuracy. *J Orofac Orthop* 2019;80:194–204.
24. Chaudhary R, Fabbri P, Leoni E, et al. Additive manufacturing by digital light processing: a review. *Prog Addit Manuf* 2023;8: 331–51.
25. Hussain MI, Xia M, Ren X, et al. Digital light processing 3D printing of ceramic materials: a review on basic concept, challenges, and applications. *Int J Adv Manuf Technol* 2024; 130:2241–67.
26. Rosa V, Silikas N, Yu B, et al. Guidance on the assessment of biocompatibility of biomaterials: fundamentals and testing considerations. *Dent Mater* 2024;40:1773–85.
27. Kreve S, dos Reis AC. Effect of surface properties of ceramic materials on bacterial adhesion: a systematic review. *J Esthetic Restor Dent* 2022;34:461–72.
28. Yue X, Suopajarvi T, Sun S, et al. High-purity lignin fractions and nanospheres rich in phenolic hydroxyl and carboxyl groups isolated with alkaline deep eutectic solvent from wheat straw. *Biore sour Technol* 2022;360:127570.
29. Gorbounov M, Halloran P, Masoudi Soltani S. Hydrophobic and hydrophilic functional groups and their impact on physical adsorption of CO<sub>2</sub> in presence of H<sub>2</sub>O: a critical review. *J CO<sub>2</sub> Util* 2024;86:102908.
30. Barberi J, Spriano S. Titanium and protein adsorption: an overview of mechanisms and effects of surface features. *Materials* 2021;14:1590.
31. Talapko J, Juzbašić M, Meštrović T, et al. Aggregatibacter actinomycetemcomitans: from the oral cavity to the heart valves. *Microorganisms* 2024;12:1451.
32. Oopath SV, Baji A, Abtahi M, et al. Nature-inspired biomimetic surfaces for controlling bacterial attachment and biofilm development. *Adv Mater Interfac* 2023;10:2201425.
33. Fiore AD, Meneghelli R, Brun P, et al. Comparison of the flexural and surface properties of milled, 3D-printed, and heat polymerized PMMA resins for denture bases: an in vitro study. *J Prosthodont Res* 2022;66:502–8.
34. Burgueño-Barris G, Camps-Font O, Figueiredo R, et al. The influence of implantoplasty on surface roughness, biofilm formation, and biocompatibility of titanium implants: a systematic review. *Int J Oral Maxillofac Implants* 2021;36: e111–9.
35. Freitas R, Duarte S, Feitosa S, et al. Physical, mechanical, and anti-biofilm formation properties of CAD-CAM milled or 3D printed denture base resins: *In vitro* analysis. *J Prosthodont* 2023;32:38–44.